Diagnostic Accuracy Study

Medicine®

OPEN

Breast lesion size assessment in mastectomy specimens

Correlation of cone-beam breast-CT, digital breast tomosynthesis and full-field digital mammography with histopathology

Susanne Wienbeck, MD[a,*], Johannes Uhlig, MD, MPH[a], Uwe Fischer, MD[b], Martin Hellriegel, MD[c], Eva von Fintel, MD[a], Dietrich Kulenkampff, MD[d], Alexey Surov, MD[e], Joachim Lotz, MD[a], Christina Perske, MD[f]

Abstract

To compare the accuracy of breast lesion size measurement of cone-beam breast-CT (CBBCT), digital breast tomosynthesis (DBT) and full-field digital mammography (FFDM).

Patients scheduled for mastectomy due to at least 1 malignant breast lesion were included. Mastectomy specimens were examined by CBBCT, DBT, FFDM, and histopathology.

A total of 94 lesions (40 patients) were included. Histopathological analyses revealed 47 malignant, 6 high-risk, and 41 benign lesions. Mean histopathological lesion size was 20.8 mm (range 2–100). Mean absolute size deviation from histopathology was largest for FFDM (5.3 ± 6.7 mm) and smallest for CBBCT 50 mA, high-resolution mode (4.3 ± 6.7 mm). Differences between imaging modalities did not reach statistical significance ($P = .85$).

All imaging methods tend to overestimate breast lesion size compared to histopathological gold standard. No significant differences were found regarding size measurements, although in tendency CBBCT showed better lesion detection and cT classification over FFDM.

Abbreviations: CBBCT = cone-beam breast computed tomography, cT = correct tumor size classification, DBT = digital breast tomosynthesis, FFDM = full-field digital mammography, HR = high-resolution, SD = standard deviation, SR = standard reconstruction, WHO = World Health Organization.

Keywords: breast cancer, cone-beam breast-CT, digital breast tomosynthesis, full-field digital mammography, mastectomy specimens

1. Introduction

Breast diseases can be broadly classified as inflammatory, benign and malignant conditions. Benign breast diseases constitute a heterogeneous group of lesions and can be subspecified as inflammatory lesions, epithelial and stromal proliferations, neoplasm, and developmental abnormalities.[1,2] Benign breast diseases, with fibroadenoma as its most common subtype, are more prevalent compared to malignant and inflammatory changes.[3] Malignant breast lesions are the most frequently diagnosed cancer in women worldwide and the leading cause of cancer-associated death with estimated 2 million new cases diagnosed worldwide in 2018.[4] Breast cancer is a heterogeneous disease, such that it may have different prognostic and therapeutic responses despite similarities in histological types, grade stage of various subtypes. Currently, there are 19 breast carcinoma subtypes according to the World Health Organization (WHO) 2003 classification, with invasive ductal carcinoma being the most common reported subtype.[5]

Accurate breast cancer size is crucial for tumor staging and an important prognostic factor in patient management.[6] Histopathological measurement of accurate breast cancer size is regarded as the gold standard, whereby therapeutic decisions heavily rely on tumor size assessment by radiological imaging.[1,7] With increasing use of breast-conserving surgery and neoadjuvant chemotherapy, the accuracy of radiological breast imaging is essential for an optimized and individualized therapy.[8] Full-field digital mammography (FFDM) is the most broadly implemented imaging modality for early detection and management of breast cancers. The diagnostic accuracy of this imaging tool shows considerable variability by breast parenchymal density, patient age, and histologic tumor type.[9] Overlying breast tissue, complicating the evaluation of the exact tumor extent, can mask further, non-calcified malignant masses in women with dense breasts.[10] Digital breast tomosynthesis

Editor: Muhammad Shahzad Aslam.

SW and JU contributed equally to this work.

The authors have no funding and conflicts of interests to disclose.

[a] Institute of Diagnostic and Interventional Radiology, University Medical Center Goettingen, [b] Diagnostic Breast Center Goettingen, [c] Department of Gynecology and Obstetrics, University Medical Center Goettingen, [d] Department of Gynecology and Obstetrics, Agaplesion Hospital Neu Bethlehem Goettingen, [e] University of Leipzig, Department of Diagnostic and Interventional Radiology, [f] Institute for Pathology, University Medical Center Goettingen, Germany.

[*] Correspondence: Susanne Wienbeck, University Medical Center Goettingen, Institute of Diagnostic and Interventional Radiology, Robert-Koch-Str. 40, 37075 Goettingen, Germany (e-mail: susanne.wienbeck@med.uni-goettingen.de).

How to cite this article: Wienbeck S, Uhlig J, Fischer U, Hellriegel M, von Fintel E, Kulenkampff D, Surov A, Lotz J, Perske C. Breast lesion size assessment in mastectomy specimens. Medicine 2019;98:37(e17082).

Received: 11 February 2019 / Received in final form: 27 June 2019 / Accepted: 14 August 2019

http://dx.doi.org/10.1097/MD.0000000000017082

(DBT) has been hypothesized to decrease this overlap, resulting in an improved distinction of benign and malignant lesions.[11,12] Despite covering the entire breast volume, DBT does not yield isotropic image resolution, since cross sectional images are reconstructed from a limited arc of movement of up to 60 degrees.[11,13]

The dedicated cone-beam breast computed tomography (CBBCT) is a flat panel detector-based system used to improve breast cancer detection and characterization.[14–19] This rapidly evolving breast-specific imaging modality exhibits unique advantages for diagnostic breast imaging, providing high-quality 3D images of the breast.[20] Despite the prognostic properties of breast cancer size and its therapeutic implications, there is no literature on the accuracy of breast lesion measurement by CBBCT in comparison to other X-ray based imaging methods.

Therefore, the aim of our study was to compare the tumor size measurement in different X-ray based imaging techniques (CBBCT, DBT, and FFDM) in mastectomy specimens using histopathological size as the gold standard.

2. Materials and methods

2.1. Study collective

This prospective, clinical study was performed in accordance to the *Declaration of Helsinki* and was approved by the institutional review board (number 2/12/14). Written informed consent was obtained from all patients before inclusion. The study was retrospectively registered with the German Clinical Trials Register (number 00012625).

The study was conducted from July 2015 to November 2016 at an University-affiliated breast imaging center and pathology department at a tertiary referral center. Patients were recruited from 2 University-affiliated breast surgery departments. Patients scheduled for mastectomy due to at least 1 biopsy-proven malignant breast lesion (masses and/ or microcalcifications) were included in the study. Exclusion criteria were architectural distortions and asymmetries. Patients with an age under 18 years and prophylactic mastectomy were also excluded.

2.2. Imaging acquisition protocol

Intraoperatively, mastectomy specimens were placed in plastic bags and immediately transferred to the Breast Imaging Center to avoid dryness and degeneration. For imaging, each specimen was positioned in a plastic container, with a volume of 1800 ml, measured 6.5 cm in height, 20.5 cm in length and 13.5 cm in width. Wall thickness amounted 1.4 mm. To ensure proper orientation of the specimen, the areola positioned uppermost in the container. The areola was positioned on the top of the plastic container and remained unchanged during the imaging procedures.

Each specimen was individually examined with CBBCT, followed by FFDM and DBT. The CBBCT system (Koning Breast CT, CBCT 1000, Koning Corporation, West Henrietta, NY) consists of a horizontal CT gantry, incorporating a mammographic X-ray tube (Rad 70, Varian Medical Systems) with a focal spot size of 0.3 mm, an X-ray flat panel detector (PaxScan 4030CB, Varian Medical Systems) mounted on the CT gantry and an ergonomically designed exam table. CBBCT scans were performed at 49 kVp, tube currents of 50 and 200 mA and with a pixel pitch of 0.388 mm (2 × 2 detector binning) resulting in a scan duration of 10 seconds for a 360° rotation.

For FFDM and DBT imaging, the same digital system was used (Senographe Essential, GE Healthcare, Chicago, IL). The DBT acquisition included 9 projection images over a ± 12.5° angle. The focal spot size was 0.3 mm for both modalities. The tube voltage for FFDM and DBT were 26–31 kVp and 29–31 kVp, respectively, depending on the specimen size. Using an automatic exposure control system, the tube currents for FFDM and DBT were 59–100 mAs and 58–65 mAs, respectively. The oriented specimens were imaged without compression. The one-view specimen radiography by FFDM and DBT were performed in cranio-caudal view.

2.3. Image analysis

All anonymized images were interpreted by a radiologist with 10 years of experience in breast imaging and 2 years of experience in dedicated CBBCT imaging on a computer workstation (Advantage Workstation 4.1, GE Healthcare, Chicago, IL). For size measurements, the greatest extent of all lesions was consecutively assessed in 3 sessions separated by a time period of 2 weeks. First the radiologist evaluated all CBBCT images, followed by FFDM and DBT images. The radiologist was blinded to the patients' information, and the pre- and postsurgical histopathological diagnosis.

Data sets from the CBBCT system were loaded into a special 3D visualization software (Visage CS Thin Client/ Server, Visage Imaging, Richmond, AUS) and evaluated on a computer workstation. The resulting 3D image sets were assessed in three orthogonal orientations (sagittal, axial and coronal) with a slice thickness of 0.5 mm. For lesion size measurement the largest extent of all lesions on imaging was assessed in the three dimensions.

During image post-processing, two different CBBCT reconstruction modes were used. For standard reconstruction (SR) images were reconstructed with a smooth kernel 273 μm voxel size. For high-resolution (HR), images were reconstructed with a sharp kernel 155 μm voxel size. The measurement of each specimen was conducted parallel to the scan direction.

After DBT acquisition, the images were processed using adaptive statistical iterative reconstruction system. The images were reconstructed with a pixel size of 100 μm and with 1.0 mm thick slices parallel to the detector plane.

2.4. Histopathological analysis

Directly after imaging, all mastectomy specimens were sent to the pathology department at a tertiary referral center. All specimens were fixed en-bloc in 4.5% neutral-buffered formalin for 24 hours and then cut sagittal into 5 mm slices. Every tumor-suspicious focus was documented regarding localization and size, photo documented and embedded in paraffin for further histopathological examinations.

For whole mount histology sections, a second fixation in 5% neutral-buffered formalin was done for another 24 hours. Samples were afterwards embedded in paraffin (Excelsior ES, Thermo Scientific), sectioned at 5 μm, and stained with Hematoxylin eosin (H&E) on an automated platform (Tissue-Tek Prisma, Sakura Finetek Germany). H&E-stained sections were visualized on an Olympus BX41 (Olympus Scientific Solutions Americas Corp., Waltham, MA). Histopathological diagnoses and measurements were digitally captured on an Olympus DP20 camera. All histopathological analyses were

performed by a board-certified pathologist with 15 years of experience on the field of breast pathology, measuring the largest lesion diameter in any dimension.

2.5. Statistical analysis

Lesion size measurements were assessed comparing the largest diameter obtained by all different breast imaging methods versus histopathological assessment in any dimension. For descriptive statistics, continuous variables are given as mean with standard deviation (SD) as measure of dispersion, and categorical variables as absolute number and percent. The assumption of normally distributed continuous variables was assessed using the Shapiro-Wilks-test. The non-normal distributed absolute difference in lesion sizes from histopathological gold standard across different imaging modalities were compared using the Kruskal-Wallis-test (non-parametric ANOVA alternative).

Bland Altman plots were utilized to visually assess over- and under-estimation of lesion size measurements across different imaging modalities from the histopathological gold standard. Correct tumor size classification (cT) was defined as the proportion of concordant size classifications between imaging modality and histopathology among all breast lesions, according to the 8th edition UICC TNM classification.[21] For comparison of correct cT classification by imaging modalities, chi-square tests were used. An alpha-level of $P \leq .05$ was chosen for to indicate statistical significance. Due to the exploratory design of this study, statistical tests were unadjusted for multiplicity and should be interpreted accordingly. All P values reported are 2-sided.

3. Results

3.1. Study collective

A total of 40 patients with 94 lesions in 40 breasts fulfilled the inclusion criteria. Figure 1 details the patient flow with inclusion and exclusion of eligible patients. The mean age was 66.7 years (SD 13.2 years). Ten patients (11%) received neoadjuvant therapy before mastectomy. In 22 patients (55%), the left breast and in 18 patients the right breast (45%) was affected. Nineteen patients presented with 1 breast lesion (48%); 21 patients (52%) had multiple breast lesions, ranging from 2 to 7 lesions per breast.

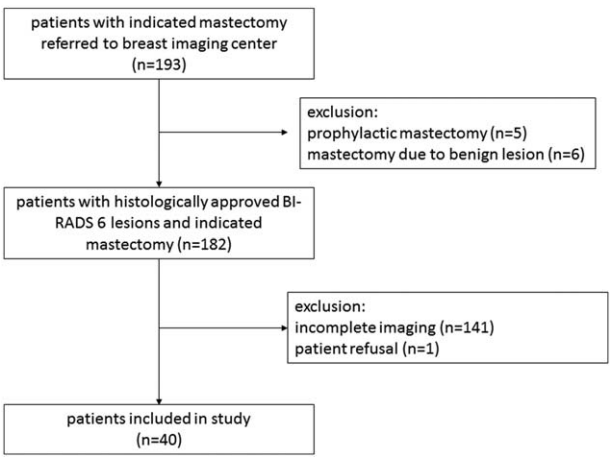

Figure 1. Flow chart including the patient's enrolment and exclusion criteria.

The majority of breast lesions presented as breast masses (n = 77, 82%). Another sixteen lesions manifested as masses with microcalcification (17%), 1 lesion presented as pure microcalcification (1%).

3.2. Histopathological results

Histopathological analyses of the mastectomy specimens revealed 47 (50%) malignant breast lesions, 6 (6.4%) high-risk lesions and 41 (43.6%) benign lesions. Among the malignant lesions, 24 were invasive ductal carcinoma (IDC), 9 IDC with associated ductal carcinoma in situ (DCIS), 4 invasive lobular carcinoma (ILC), 2 micropapillary carcinomas, 1 mucinous carcinoma (MC) and 7 DCIS. Among the 6 high-risk lesions, intraductal papillomas (n = 5), and atypical ductal hyperplasia (ADH) (n = 1) were diagnosed. Various benign lesions (n = 41 lesions, 43.6%) were diagnosed, of which intramammary lymph nodes (n = 20, 21.2%) and fibrosis (n = 10, 10.6%) were the most common. For all analyses, high-risk lesions were included in the group of malignant lesions. Table 1 summarizes histopathological results of all breast lesions.

3.3. Lesion size agreement between histopathological gold standard and imaging modalities

The mean lesion size determined by histopathology was 20.8 mm (range 2–100 mm). Mean lesion size determined by CBBCT was 23.4 to 23.7 mm depending on reconstruction mode and tube currents, by FFDM was 26.7 mm (SD 24.8 mm) and by DBT was 23.5 mm (SD 22.6 mm).

For CBBCT, mean lesion size was for images acquired with 50 mA, SR mode 23.6 mm (SD 22.5 mm), and for 50 mA, HR mode 23.4 mm (SD 22.2 mm). For images acquired with 200 mA, SR mode, mean lesion size was 23.7 mm (SD 22.3 mm), and for 200 mA, HR mode 23.5 mm (SD 21.9 mm). Figure 2 depicts largest lesion size as determined by the different modalities, showing a right-skewed distribution. Shapiro-Wilks tests confirmed non-normal distribution of size measurements for all modalities (each $P < .001$).

Table 1

Diagnosis of 94 histological proven lesions included in the study collective.

Histologic results	Lesions (n = 94)	(%)
Benign (n = 41)		
Fibrocystic changes	3	3.2
Fibrosis mammae	10	10.6
Sclerosing adenosis	1	1.1
Fibroadenoma	4	4.3
Fat necrosis	1	1.1
Cyst	2	2.1
Lymph node	20	21.2
High-risk (n = 6)		
Papilloma	5	5.3
ADH	1	1.1
Malignant (n = 47)		
DCIS	7	7.4
IDC	24	25.5
IDC + DCIS	9	9.6
ILC	4	4.3
Others	3	3.2

ADH = atypical ductal hyperplasia, DCIS = ductal carcinoma in situ, IDC = invasive ductal carcinoma, ILC = invasive lobular carcinoma, n = number.

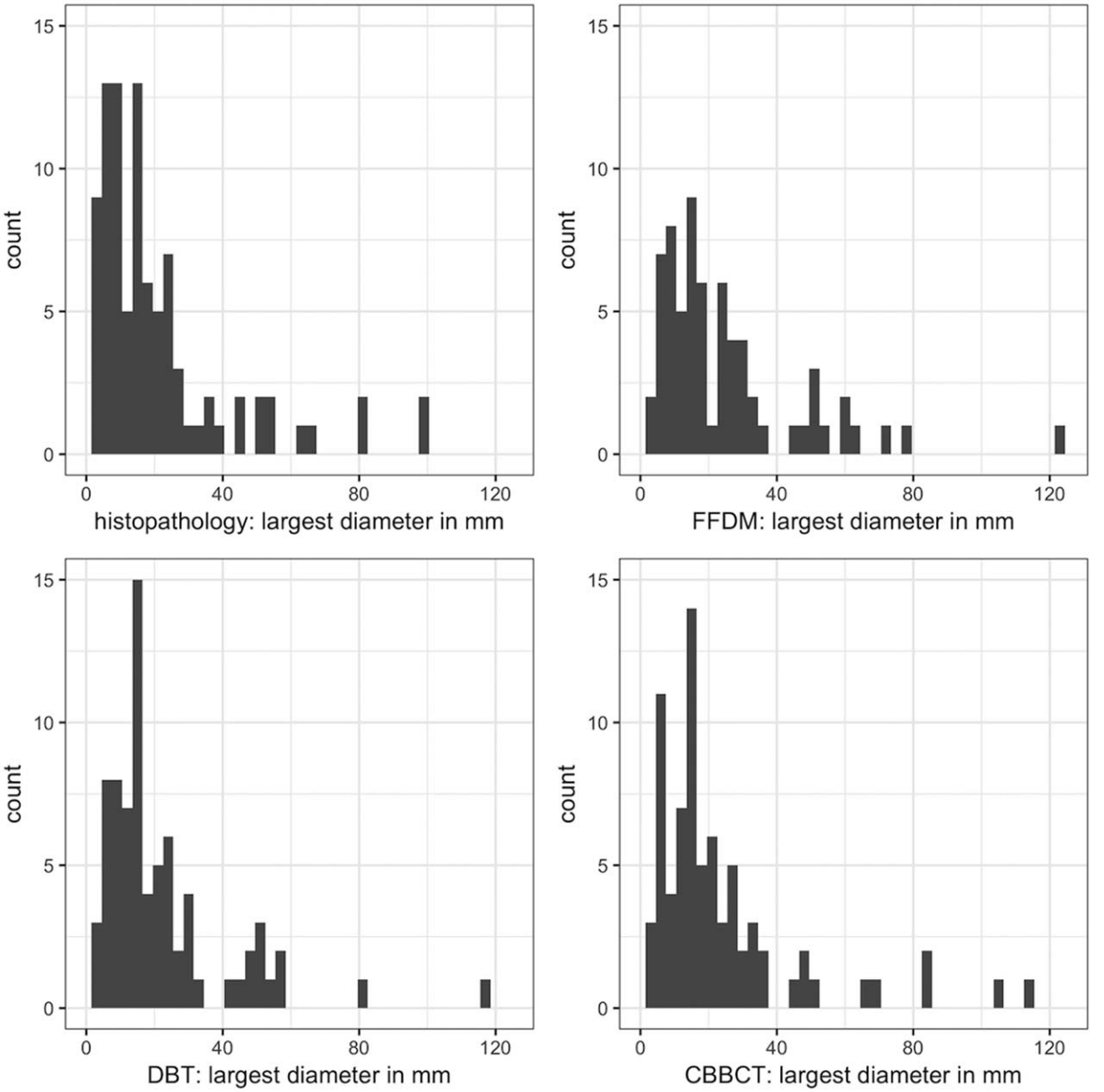

Figure 2. Histograms of largest breast lesion diameter measured by histopathology, full-field digital mammography, digital breast tomosynthesis and CBBCT. For visualization purpose, the average diameter of the 4 different CBBCT reconstruction modes and tube current was plotted. CBBCT = cone-beam breast-CT.

Lesion size measurements by different imaging modalities yielded no statistically significant difference ($P = .55$).

Mean absolute deviation from histopathology was largest for FFDM (mean 5.3 mm, SD 6.5 mm), and smallest for CBBCT 50 mA, HR mode (mean 4.3 mm, SD 6.7 mm). All modalities yielded non-normal distribution of lesion size deviation from histopathology (each Shapiro-Wilks $P < .001$). There was no statistically significant difference in lesion size deviations from histopathology. Lesion size measurement and deviation from histopathology are summarized in Table 2.

Figure 3 shows Bland-Altman plots comparing lesion sizes by imaging modalities to histopathology for low- and high-density breasts. All imaging modalities tended to overestimate lesion size compared to histopathology. For FFDM, a larger tendency towards higher overestimation with increasing lesion size was noted, as indicated by the associated regression line with confidence intervals. For both large and small breast lesions, CBBCT consistently showed smaller absolute size deviation from histopathological gold standard, as summarized in Table 2.

Furthermore, Table 3 shows the detection and correct size classification of breast lesions by various imaging modalities with the histopathological gold standard. CBBCT with 50 mA, SR mode, yielded the highest concordance in detection and correct size classification with histopathology (71.3%), although differences in detection rate across imaging modalities did not reach statistical significance ($P = .78$). An example of a malignant mass in the 3 imaging modalities and the histopathology result as the gold standard is shown in Figures 4 and 5.

Table 2

Lesion size by histopathological gold standard and different imaging modalities.

Modality	Mean (SD) lesion size in mm	*P* value	Mean (SD) absolute size deviation in mm from histopathology	Mean (SD) absolute size deviation in mm for small lesions (<15mm)	Mean (SD) absolute size deviation in mm for large lesions (>15mm)
Histopathology	20.8 (20.6)	Reference	–	–	–
FFDM	26.7 (24.8)	.077	5.3 (6.5)	3.1 (3.8)	7.1 (7.7)
DBT	23.5 (22.6)	.393	4.9 (6.2)	3.3 (3.8)	6.3 (7.3)
CBBCT					
50 mA, SR	23.6 (22.5)	.375	4.4 (6.6)	2.6 (2.3)	6.0 (8.6)
50 mA, HR	23.4 (22.2.)	.406	4.3 (6.7)	2.4 (2.2)	6.1 (8.7)
200 mA, SR	23.7 (22.3)	.356	4.3 (6.7)	2.5 (2.3)	6.0 (8.7)
200 mA, HR	23.5 (21.9)	.385	4.4 (6.8)	2.4 (2.4)	6.1 (8.7)

CBBCT = cone-beam breast-CT, DBT = digital breast tomosynthesis, FFDM = full-field digital mammography, HR = high-resolution reconstruction, mA = milliampere, SD = standard deviation, SR = standard reconstruction.

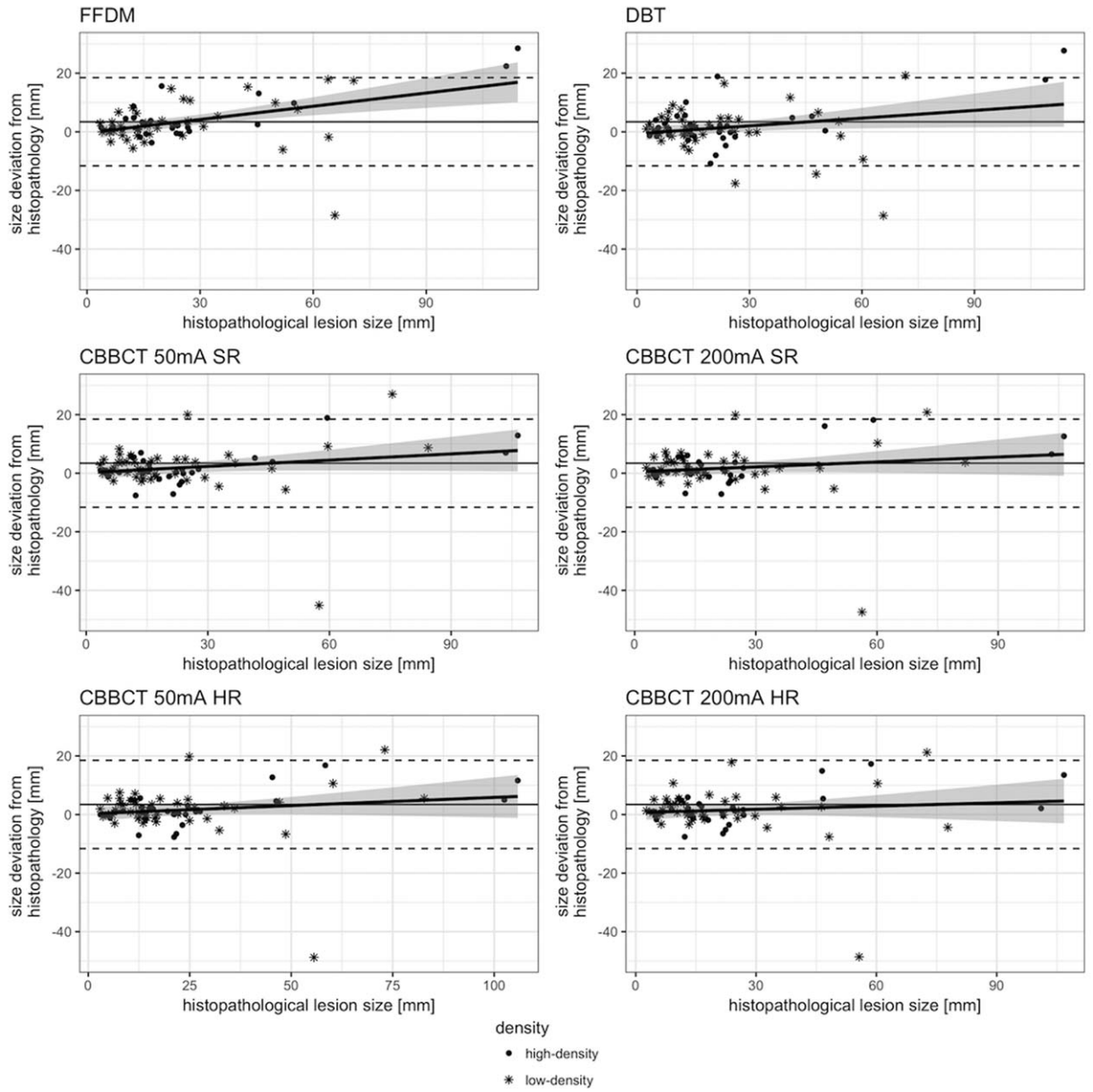

Figure 3. Bland-Altman plots by breast density (dot: lesions in high-density breasts; asterisk: lesions in low-density breasts). Deviation of lesion size measured by full-field digital mammography, digital breast tomosynthesis and cone-beam breast-CT from histopathological gold standard was plotted. Horizontal line indicates mean deviation and dotted horizontal lines 95% confidence intervals for deviation. A bold regression line with corresponding 95% confidence limits in grey was added. CBBCT = cone-beam breast-CT, DBT = digital breast tomosynthesis, FFDM = full-field digital mammography, HR = high-resolution reconstruction, SR = standard reconstruction.

Table 3

Agreement between tumor staging on imaging and pathology of measurable tumors.

		Histopathology			Correct cT classification
		pT1	pT2	pT3	all breasts
FFDM	cT1	**37**	–	–	
	cT2	4	**14**	1	58/94, 61.7%
	cT3	–	4	**7**	
DBT	cT1	**41**	3	–	
	cT2	5	**16**	1	64/94, 68.1%
	cT3	–	2	**7**	
CBBCT 50 mA, SR mode	cT1	**44**	2	–	
	cT2	3	**18**	2	67/94, 71.3%
	cT3	–	1	**5**	
CBBCT 50 mA, HR mode	cT1	**43**	2	–	
	cT2	4	**17**	2	65/94, 69.1%
	cT3	–	2	**5**	
CBBCT 200 mA, SR mode	cT1	**43**	1	–	
	cT2	3	**18**	2	66/94, 70.2%
	cT3	–	2	**5**	
CBBCT 200 mA, HR mode	cT1	**43**	2	–	
	cT2	3	**17**	2	65/94, 69.1%
	cT3	–	2	**5**	

c = clinical stage, CBBCT = cone-beam breast-CT, cT = clinical tumor, DBT = digital breast tomosynthesis, FFDM = full-field digital mammography, HR = high-resolution reconstruction, mA = milliampere, p = pathologic stage, SR = standard reconstruction, T1 = includes tumors ≤ 20 mm in diameter, T2 = includes tumors > 20 mm and ≤ 50 mm, T3 = includes tumors > 50 mm.

4. Discussion

Precise size measurement of tumorous lesions is crucial, especially for patients with histological proved breast cancer. Accurate lesion size measurement is essential for optimal treatment decisions and evaluation of patient's response to neoadjuvant chemotherapy and a relevant prognostic factor.[6]

Previously, different imaging modalities were analyzed for tumor size measurement. According to the literature, there are numerous studies comparing FFDM, ultrasound (US) and MRI between them and separately, with discrepant results. Some studies report that US is better than FFDM.[22,23] Other studies report that MRI is superior to that of the FFDM and the US.[7,24] But in the most recent studies MRI overestimates tumor size and measurements obtained with US and FFDM are more accurate independently of breast density.[7,22,25,26]

Nevertheless, MRI for breast specimen imaging is still far away from implementation in a clinic setting because of the usefulness of high field MRI scanners and the harder operation and longer imaging time compared to radiography.[27] It showed promising results for intraoperative margin assessment but with a lack in visualization of DCIS lesions without an invasive component.[27]

DBT during intraoperative specimen evaluation was for lesion detection and characterization higher than for FFDM.[28] DBT may reduce the need allocated specimen ultrasonography in patients with dense breast tissue.

In the present study, we analyzed only different X-ray based modalities, to evaluate the accuracy of the measured tumor size for different histological breast lesions. In this context intraoperative specimen radiography is the method of choice to evaluate the resection margins.[29–31]

In our study, we showed that FFDM, DBT, and CBBCT consistently overestimate lesions size, and that this overestimation tends to increase for larger breast lesions. Despite missing statistical significance, CBBCT yielded smaller absolute size deviations from histopathological gold standard.

Among all imaging modalities, CBBCT with a tube current of 50 mA, SR mode demonstrated highest concordance in detection and correct cT classification with histopathology. Although our findings did not reach statistical significance difference of up to 9.6% in correct cT classification of malignant breast lesions for CBBCT versus FFDM seem clinically relevant.

So far, only 2 authors described initial experiences concerning CBBCT imaging of mastectomy specimens with the CBBCT scanner used in our study.[32,33] Two other studies reported on specimen evaluation with a photon-counting breast computed tomography (pcBCT).[34,35] Our study is the first one to focus on breast lesions size measurement in mastectomy specimens with evaluating different imaging modalities, including CBBCT, in comparison to histopathology as the gold standard.

In concordance to 1 study comparing DBT and FFDM, we observed an overestimation of tumor size with all modalities.[8] Also CBBCT, independent of reconstruction mode and tube current, showed an overestimation of breast lesion size in comparison to histopathology. Potentially, the breast tissue could have shrunken during the following histopathological processes, as proposed by other authors.[36] Further, slices chosen for pathological assessment might have not contained the maximum tumor extent.[37]

In contrast, most of the previous studies with FFDM and US have underestimated the true lesion size.[23,36–38] Conservative measurements of the lesions' extent excluding spiculated periphery with both modalities might underlie these findings.[36,37] Surprisingly, we found an overestimation of lesions size with all modalities, although spicules of stellated lesions were excluded in our measurements as well.

Studies focusing on the accuracy of DBT concluded that DBT is superior to FFDM for assessment of breast lesion size and stage.[8,37] Both studies reported a higher agreement of lesion detection and classification between DBT and pathology in comparison to FFDM and pathology.[8,37] Rößler et al[34] recently reported on pcBCT outperforming FFDM and DBT in the detection of microcalcifications and mass lesions. In tendency, our findings agree with Rößler et al, since lesion detection and correct cT classification was best for CBBCT, although differences did not reach statistical significance.

Our study has several limitations. Due to the single reader study-design, the interobserver variability of lesion size measurement and image interpretation concerning breast density could not be evaluated. Secondly, breast imaging modalities were acquired and read in a non-random sequence, which might have favored assessment of one modality. Third, we selected patients with at least 1 malignant breast lesion scheduled for mastectomy, which might have biased lesion assessment. Fourth the reader could expect larger breast lesions, because a mastectomy was indicated. The proposed methods to overcome this limitation, mainly separate interpretation of both breasts for the same patient, could not been implemented in our study due to the nature of mastectomies. Further, lesion margin status and histologic subtype might both influence size measurement but were not assessed in our study. Finally, due to the ex-vivo fixation of mastectomy specimens in our study, only the cranio-caudal view for FFDM and DBT was assessed.

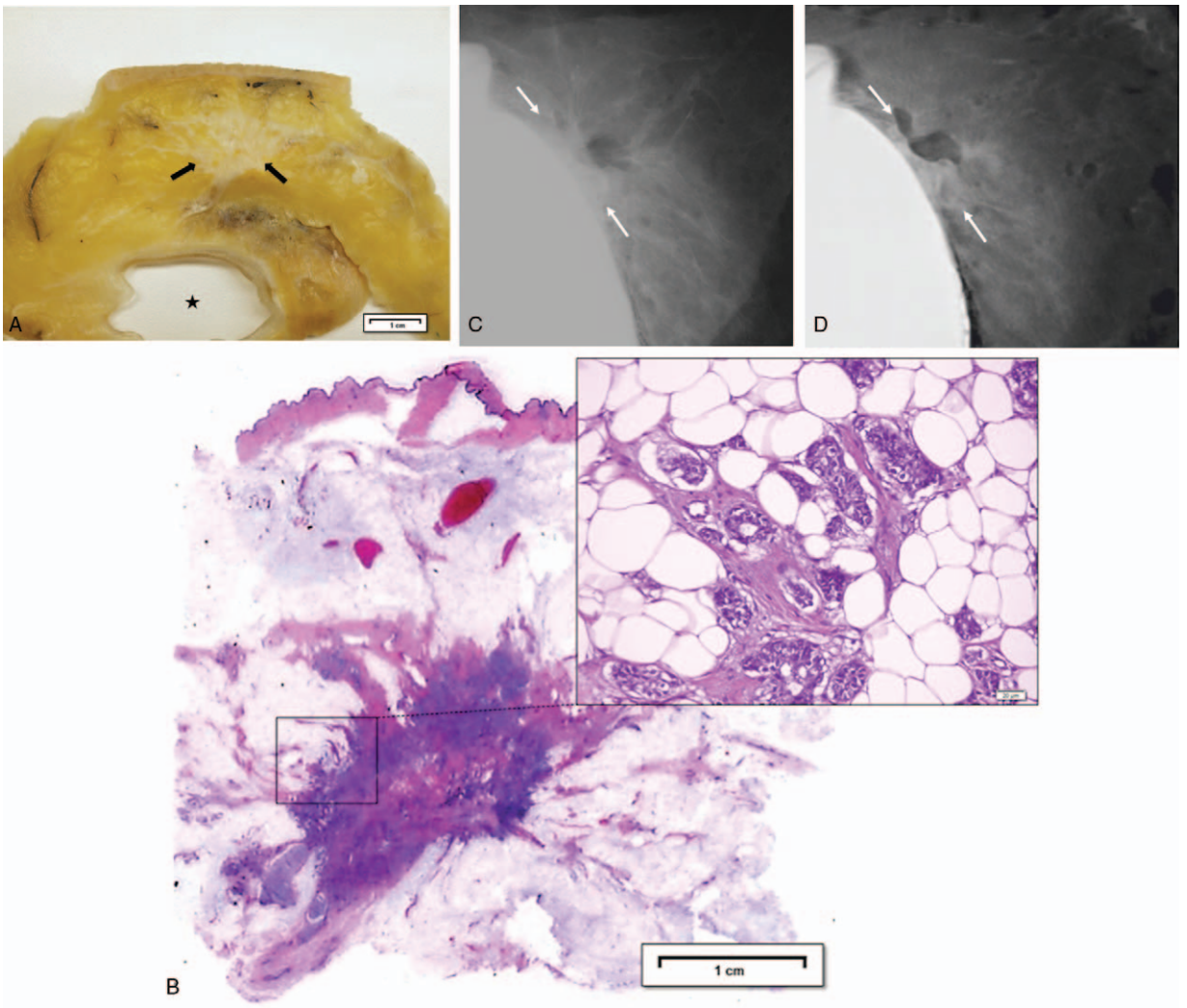

Figure 4. A 60-year old woman with invasive ductal carcinoma, grade 2 with American College of Radiology density type b who underwent mastectomy. (A) Macroscopic finding after slicing the mastectomy specimen. The pathology determined a 20 mm large indurated mass with spiculated diffuse margins (black arrows). Applied breast implantat for cosmetic reasons (star). Another 5 papillomas in the same breast (not illustrated). (B) Large-format/whole mount histology section and higher magnification (200×) showing an unifocal invasive ductal carcinoma, grade 2 (H&E). (C) For the lesion characteristic a spiculated mass with a mean size of 24.7 mm (with arrows) was seen directly in contact to the breast implantat with FFDM. (D) The mass measured 26.1 mm with digital breast tomosynthesis (slice thickness 0.5 mm).

Our study has several strengths. First, a comparably large number of mastectomy specimens and breast lesions were assessed. Lesion size and histological subtype varied, enhancing the generalizability of our results. Further, various CBBCT reconstruction modes and tube currents were assessed showing consistent results.

5. Conclusion

FFDM, DBT, and CBBCT tend to overestimate breast lesion size compared to histopathological gold standard. No significant differences were found regarding size measurements, although in tendency CBBCT showed better lesion detection and cT classification over FFDM. CBBCT demonstrates its advantage in determining the 3D position of a lesion, which could be a potential clinical application in future practices of breast imaging.

Acknowledgments

The authors gratefully acknowledge the team of the Diagnostic Breast Center Goettingen, Germany and Klaus-Peter Hermann, Germany for their continuous and excellent support. Special thanks go to Peter Dziuban, University Medical Center Göttingen for his great contributions to specimen transport.

Author contributions

Conceptualization: Susanne Wienbeck.
Data curation: Susanne Wienbeck, Christina Perske.
Formal analysis: Susanne Wienbeck, Johannes Uhlig, Uwe Fischer, Alexey Surov, Christina Perske.
Investigation: Susanne Wienbeck.
Methodology: Susanne Wienbeck.
Project administration: Susanne Wienbeck.
Resources: Uwe Fischer, Martin Hellriegel, Dietrich Kulenkampff, Joachim Lotz.
Supervision: Susanne Wienbeck.
Visualization: Johannes Uhlig, Christina Perske.
Writing – original draft: Susanne Wienbeck, Johannes Uhlig, Christina Perske.

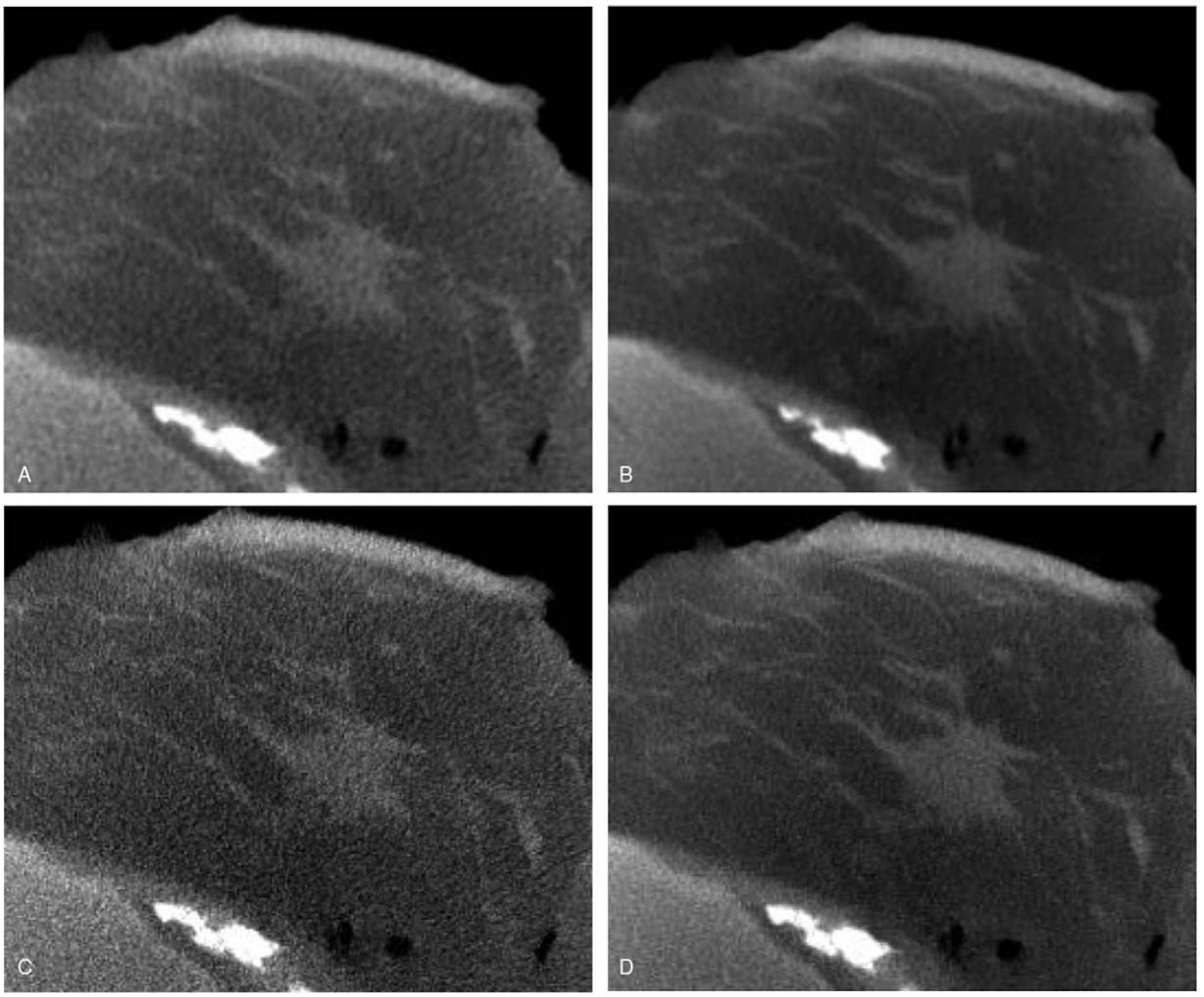

Figure 5. For the same mastectomy specimen a CBBCT scan demonstrated the mass lesion in coronal view with a slice thickness of 0.5 mm and 2 different tube currents (50 and 200 mA) and reconstruction algorithm (SR / HR mode). (A) CBBCT 50 mA, SR mode: The mean size of the lesion was 23.6 mm. (B) CBBCT 50 mA, HR mode: The mean size of the lesion was 23.9 mm. (C) CBBCT 200 mA, SR mode: The mean size of the lesion was 23.9 mm. (D) CBBCT 200 mA, HR mode: The mean size of the lesion was 24.7 mm. For all CBBCT images an overestimation of lesion size was seen. The mass was more clearly detected on CBBCT with 50 mA, SR mode. CBBCT = cone-beam breast computed tomography, HR = high-resolution reconstruction, SR = standard reconstruction.

Writing – review & editing: Susanne Wienbeck, Johannes Uhlig, Uwe Fischer, Martin Hellriegel, Eva von Fintel, Dietrich Kulenkampff, Alexey Surov, Joachim Lotz, Christina Perske.

References

[1] Guray M, Sahin AA. Benign breast diseases: classification, diagnosis, and management. Oncologist 2006;11:435–49.
[2] Aslam HM, Saleem S, Shaikh HA, et al. Clinico- pathological profile of patients with breast diseases. Diagn Pathol 2013;8:77.
[3] Olu-Eddo AN, Ugiagbe EE. Benign breast lesions in an African population: a 25-year histopathological review of 1864 cases. Niger Med J 2011;52:211–6.
[4] Bray F, Ferlay J, Soerjomataram I, et al. Global cancer statistics 2018: GLOBOCAN estimates of incidence and mortality worldwide for 36 cancers in 185 countries. CA Cancer J Clin 2018;68:394–424.
[5] Cakir A, Gonul II, Uluoglu O. A comprehensive morphological study for basal-like breast carcinomas with comparison to nonbasal-like carcinomas. Diagn Pathol 2012;7:145.
[6] Michaelson JS, Silverstein M, Sgroi D, et al. The effect of tumor size and lymph node status on breast carcinoma lethality. Cancer 2003; 98:2133–43.
[7] Gruber IV, Rueckert M, Kagan KO, et al. Measurement of tumour size with mammography, sonography and magnetic resonance imaging as compared to histological tumour size in primary breast cancer. BMC Cancer 2013;13:328.
[8] Seo N, Kim HH, Shin HJ, et al. Digital breast tomosynthesis versus full-field digital mammography: comparison of the accuracy of lesion measurement and characterization using specimens. Acta Radiol 2014;55:661–7.
[9] Heine JJ, Malhotra P. Mammographic tissue, breast cancer risk, serial image analysis, and digital mammography. Part 2. Serial breast tissue change and related temporal influences. Acad Radiol 2002;9:317–35.
[10] Boyd NF, Guo H, Martin LJ, et al. Mammographic density and the risk and detection of breast cancer. N Engl J Med 2007;356:227–36.
[11] Helvie MA. Digital mammography imaging: breast tomosynthesis and advanced applications. Radiol Clin North Am 2010;48:917–29.
[12] Andersson I, Ikeda DM, Zackrisson S, et al. Breast tomosynthesis and digital mammography: a comparison of breast cancer visibility and BIRADS classification in a population of cancers with subtle mammographic findings. Eur Radiol 2008;18:2817–25.
[13] Kopans DB. Digital breast tomosynthesis from concept to clinical care. AJR. AJR Am J Roentgenol 2014;202:299–308.
[14] Lindfors KK, Boone JM, Nelson TR, et al. Dedicated breast CT: initial clinical experience. Radiology 2008;246:725–33.

[15] O'Connell A, Conover DL, Zhang Y, et al. Cone-beam CT for breast imaging: radiation dose, breast coverage, and image quality. AJR. Am J Roentgenol 2010;195:496–509.
[16] O'Connell AM, Kawakyu-O'Connor D. Dedicated cone-beam breast computed tomography and diagnostic mammography: comparison of radiation dose, patient comfort, and qualitative review of imaging findings in BI-RADS 4 and 5 lesions. J Clin Imaging Sci 2012;2:7.
[17] Lindfors KK, Boone JM, Newell MS, et al. Dedicated breast computed tomography: the optimal cross-sectional imaging solution? Radiol Clin North Am 2010;48:1043–54.
[18] Zhao B, Zhang X, Cai W, et al. Cone beam breast CT with multiplanar and three dimensional visualization in differentiating breast masses compared with mammography. Eur J Radiol 2015;84:48–53.
[19] He N, Wu YP, Kong Y, et al. The utility of breast cone-beam computed tomography, ultrasound, and digital mammography for detecting malignant breast tumors: a prospective study with 212 patients. Eur J Radiol 2016;85:392–403.
[20] Sarno A, Mettivier G, Russo P. Dedicated breast computed tomography: basic aspects. Med Phys 2015;42:2786–804.
[21] Brierley JD, Gospodarowicz MK, Wittekind C. The TNM classification of malignant tumours. 8th Ed. Oxford: Wiley Blackwell; 2017.
[22] Leddy R, Irshad A, Metcalfe A, et al. Comparative accuracy of preoperative tumor size assessment on mammography, sonography, and MRI: Is the accuracy affected by breast density or cancer subtype? J Clin Ultrasound 2016;44:17–25.
[23] Hieken TJ, Harrison J, Herreros J, et al. Correlating sonography, mammography, and pathology in the assessment of breast cancer size. Am J Surg 2001;182:351–4.
[24] Wasif N, Garreau J, Terando A, et al. MRI versus ultrasonography and mammography for preoperative assessment of breast cancer. Am Surg 2009;75:970–5.
[25] Houssami N, Turner R, Morrow M. Preoperative magnetic resonance imaging in breast cancer: meta-analysis of surgical outcomes. Ann Surg 2013;257:249–55.
[26] Behjatnia B, Sim J, Bassett LW, et al. Does size matter? Comparison study between MRI, gross, and microscopic tumor sizes in breast cancer in lumpectomy specimens. Int J Clin Exp Pathol 2010;3:303–9.
[27] Abe H, Shimauchi A, Fan X, et al. Comparing post-operative human breast specimen radiograph and MRI in lesion margin and volume assessment. J Appl Clin Med Phys 2012;13:3802.
[28] Polat YD, Taskin F, Cildag MB, et al. The role of tomosynthesis in intraoperative specimen evaluation. Breast J 2018;24:992–6.
[29] Britton PD, Sonoda LI, Yamamoto AK, et al. Breast surgical specimen radiographs: how reliable are they? Eur J Radiol 2011;79:245–9.
[30] Angarita FA, Nadler A, Zerhouni S, et al. Perioperative measures to optimize margin clearance in breast conserving surgery. Surg Oncol 2014;23:81–91.
[31] Amer HA, Schmitzberger F, Ingold-Heppner B, et al. Digital breast tomosynthesis versus full-field digital mammography-Which modality provides more accurate prediction of margin status in specimen radiography? Eur J Radiol 2017;93:258–64.
[32] Yao J, Shaw C, Lai CJ, et al. Cone beam CT for determining breast cancer margin: an initial experience and its comparison with mammography and specimen radiograph. Int J Clin Exp Med 2015;8:15206–13.
[33] Yang WT, Carkaci S, Chen L, et al. Dedicated cone-beam breast CT: feasibility study with surgical mastectomy specimens. AJR Am J Roentgenol 2007;189:1312–5.
[34] Rossler AC, Kalender W, Kolditz D, et al. Performance of Photon-counting breast computed tomography, digital mammography, and digital breast tomosynthesis in evaluating breast specimens. Acad Radiol 2017;24:184–90.
[35] Kalender WA, Kolditz D, Steiding C, et al. Technical feasibility proof for high-resolution low-dose photon-counting CT of the breast. Eur Radiol 2017;27:1081–6.
[36] Bosch AM, Kessels AG, Beets GL, et al. Preoperative estimation of the pathological breast tumour size by physical examination, mammography and ultrasound: a prospective study on 105 invasive tumours. Eur J Radiol 2003;48:285–92.
[37] Fornvik D, Zackrisson S, Ljungberg O, et al. Breast tomosynthesis: accuracy of tumor measurement compared with digital mammography and ultrasonography. Acta Radiol 2010;51:240–7.
[38] Pritt B, Ashikaga T, Oppenheimer RG, et al. Influence of breast cancer histology on the relationship between ultrasound and pathology tumor size measurements. Mod Pathol 2004;17:905–10.